Ring currents and correlation transition in regular annulenes

Y. Anusooya and Z. G. Soos

Department of Chemistry, Princeton University, Princeton, NJ 08544, USA

Diamagnetic ring currents in regular $4n+2$ annulenes and paramagnetic currents in $4n$ annulenes attenuate abruptly with increasing electron–electron correlation $V(R)$. The crossover to vanishing ring currents sharpens with increasing ring size N and reflects spin-charge separation in half-filled Hubbard or Pariser–Parri–Pople models when the on-site repulsion U exceeds the bandwidth $4t$. Diamagnetic ground-state and paramagnetic excited-states contributions to ring currents cancel exactly to order $(t/U)^3$ for any $V(R)$ that reduces to a Heisenberg antiferromagnetic spin chain for $U \gg t$. The PPP model with molecular parameters accounts for decreasing ring currents beyond 18-annulene, for large ring currents in charged annulenes, and for π-electronic excitations of pyracylene, a nonalternant hydrocarbon containing both paramagnetic and diamagnetic rings. The correlation transition from a diamagnetic to nonmagnetic ground state resembles a Mott or metal–insulator transition in half-filled systems, although ring currents are compatible with finite energy gaps.

HÜCKEL theory is an elegant general approach to conjugated molecules that parallels tight-binding band theory. Single-particle descriptions are convenient and successful, especially for ground-state properties, but localization, spin-charge separation or excitations require electron–electron correlation $V(R)$. Hubbard and related solid-state models follow the evolution of ground-state properties or responses with increasing e–e correlations such as $U>0$ or V for two electrons at the same or adjacent sites, respectively; U and V are typically adjustable in diverse low-dimensional systems. The Pariser–Parr–Pople (PPP) model for π–π^* spectra of conjugated hydrocarbons exploits their similarities to fix $V(R)$ in advance and make possible spectroscopic predictions. Even and odd-parity excitations, intensities and nonlinear optical responses agree with experiment for *exact* PPP results[1,2], including the nonalternant hydrocarbon, pyracylene, treated below. Although used in entirely different contexts, Hubbard, PPP and related quantum cell models are similar ways of adding $V(R)$ to systems with electron transfer t between adjacent sites.

N-site rings with $N_e=N$ electrons have closed-shell ground states for $N=4n+2$ in Hückel theory, open shells for $N=4n$. Benzene ($N=6$) and $4n+2$ annulenes illustrate aromatic stabilization, while cyclobutadiene or cyclooctatetraene are antiaromatic and subject to Jahn–Teller distortion. Hückel's $4n/4n+2$ rule follows directly for noninteracting π-electrons and gives far reaching insights into conjugation[3]. The model is a regular planar N-sided polygon. Longuet-Higgins and Salem[4] showed that $4n+2$ π-systems become unstable to alternation with increasing N, as follows from Peierls' analysis of half-filled bands. Ground-state alternation in polyenes and polyacetylene has been extensively discussed[5] and quantitative comparisons require a full analysis. Physical organic chemists introduce reference states to obtain aromatic stabilization systematically in molecules. In extended systems, the problem is to extract contributions of π-electrons or frontier orbitals from an (often large) core background. Modeling specific contributions or partitioning observations is instructive but rarely unique.

We restrict discussion to π-electrons and regular annulenes with C_N rotational symmetry, in the spirit of the $4n/4n+2$ rule or London diamagnetism[6], and consider the effects of e–e correlation on ring currents I_N induced by a magnetic field H normal to the molecular plane. We start with the generic problem of increasing $U/4t$ in half-filled systems and show that both diamagnetic I_N in $4n+2$ rings and paramagnetic I_N in $4n$ rings are suppressed for $U \gg t$. Reduced ring currents are consistent with a metal–insulator transition in the infinite chain as the bandwidth $4t$ decreases. The differences are that finite systems support ring currents and that the currents are due to magnetic rather than electric fields. We report crossovers that sharpen with N for Hubbard, PPP or any quantum-cell model that reduces to a Heisenberg antiferromagnetic chain in the limit of strong correlations. PPP results with molecular parameters bear directly on I_N observed as NMR shifts. Magnetic resonance is a powerful modern microscopic method for probing anisotropic magnetic susceptibilities that initially relied on macroscopic crystals[7].

Ring currents in correlated models

We consider a polygon with C_N symmetry in the xy plane, $N_e=N$ electrons, and gauge origin at the center.

*For correspondence.

The integrals t acquire[8] a phase factor $f = eSH/\hbar cN$ in a magnetic field H along the z-axis, where $S = (NR^2/4)\cot(\pi/N)$ is the area for side R, e is the charge and c the speed of light. The Hamiltonian is[9]

$$H = -t\sum_{p\sigma}[a^{+}_{p\sigma}a_{p+1\sigma}\exp(if) + a^{+}_{p+1\sigma}a_{p\sigma}\exp(-if)] + V(R), \quad (1)$$

with $t > 0$ and opposite phases for electron transfer to the right and left. The potential is

$$V(R) = \sum_{p} Un_p(n_p - 1)/2 + \sum_{p\neq p'} V_{pp'}(n_p - 1)(n_{p'} - 1)/2 \quad (2)$$

and depends exclusively on the π-electron number operators, $n_p = 0$, 1 or 2. The first term is the Hubbard model. The Ohno potential[10], $V_{pp'} = e^2/(R^2_{pp'} + e^4/U^2)^{1/2}$ with $U = 11.26$ eV, is a frequent choice for PPP models[1]. Other choices for $V_{pp'}$ yield extended Hubbard models with spin-independent $V(R)$. Since the field appears exclusively in the Hückel part, we follow Salem's detailed single-particle treatment[8] of magnetic properties except for using correlated states.

The exact ground-state energy per site of eq. (1) at $H = 0$ is

$$\varepsilon_N(z) = E_0(z, N)/N, \quad (3)$$

where $z = U/4t$ is a correlation index that ranges from noninteracting particles at $z = 0$ to strong correlations at $z > 1$ for any $V(R)$. We obtain $\varepsilon_N(z)$ numerically for finite N and rely on exact results for infinite Hubbard or spin chains. The exact ground state, $|G(z, N)\rangle$, is a nondegenerate singlet for even $N = N_e$ and $z > 0$, but is degenerate in $4n$ Hückel rings. Exact $H = 0$ excited states $|k(z, N)\rangle$ at $E_k(z, N)$ are restricted to oligomers, currently[11] $N = 16$ or perhaps 18 on a workstation. This corresponds to over 34 and 350 million singlet functions, respectively. The number of Slater determinants with $S_z = 0$ is considerably larger[2], $N!/(N/2)!$

Magnetic properties of eq. (1) are second-order corrections, $-f^2E_2/2$, in H to $E_0(z, N)$ for nondegenerate $|G(z, N)\rangle$, and $f \sim 10^{-4}$ is typically very small[8]. Since the static susceptibility χ is proportional to E_2, the system is diamagnetic when $E_2 < 0$, paramagnetic when $E_2 > 0$. Assuming that χ is due to a ring current I_N along the periphery, we have[8]

$$I_N(z) = \frac{He^2S}{\hbar^2N^2}E_2(z, N). \quad (4)$$

The $z = 0$ expression holds for any $V(R)$ in eq. (1) because the field modifies only the transfer integrals in quantum cell models. Since S/N^2 is $(R^2/4N)\cot(\pi/N) \sim R^2/4\pi$, ring currents are extensive and proportional to E_2. The proportionality constant is required for experimental comparisons, but not our study of size and correlation dependencies. $I_N(z)$ and $E_2(z, N)$ are used interchangeably below.

We expand eq. (1) in f and retain contributions up to H^2 to obtain the formal solution[9],

$$E_2(z, N) = -t\langle G(z, N)|\nu_+|G(z, N)\rangle + 2t^2\sum_k |\langle k(z, N)|\nu_-|G(z, N)\rangle|^2/(E_k - E_0)$$

$$\nu_\pm(z, N) \equiv \sum_{p\sigma}(a^{+}_{p\sigma}a_{p+1\sigma} \pm a^{+}_{p+1\sigma}a_{p\sigma}), \quad (5)$$

where we have used the fact that $\langle G|\nu_-|G\rangle = 0$. The ν_+ expectation value is the π-bond order and is always diamagnetic; it corresponds to ground-state precession. The ν_- contribution from excited states is positive and is an example of Van Vleck paramagnetism; ring currents due to excited states reinforce H. The current vanishes or reverses at $E_2 = 0$.

We evaluate the sum in eq. (5) for oligomers using correction vectors[12,9] to obtain $E_2(z, N)$ or $I_N(z)$. Figure 1 depicts exact E_2 for Hubbard and PPP models with increasing $z = U/4t$. We find that $4n + 2$ and $4n$ annulenes are diamagnetic and paramagnetic, respectively, and that I_N attenuates sharply for $z > 1$. There are striking crossovers in the $4n + 2$ series; diamagnetic I_N increase with N at small z, decrease with N for $z > 1$. The atomic limit of half-filled Hubbard or PPP systems rationalizes small currents for $z \gg 1$, when eq. (1) reduces to a Heisenberg chain with only spin degrees of freedom. The abrupt changes in Figure 1 point to strong and unanticipated cancellations in E_2. To underscore this, we compare in Figure 2 *magnitudes* of the ν_+ and ν_- terms for a 14-site PPP ring. The diamagnetic term dominates at small z; the two terms become equal in magnitude at $z > 1$, and then decrease gently as $1/z$ with increasing correlation. We associate the suppression of I_N with a transition to a localized state and argue below that the result is general.

Hückel ($z = 0$) results are elementary. To order N^{-2}, we have

$$\varepsilon_N(0) = -\frac{4t}{\pi}\left(1 + \frac{a\pi^2}{6N^2}\right), \quad (6)$$

with $a = 1$ for $N = 4n + 2$ and $a = -2$ for $N = 4n$. The N^{-2} term is aromatic stabilization in $4n + 2$ rings or antiaromatic destabilization in $4n$ rings relative to the infinite chain. The ν_+ expectation value in eq. (5) is simply $-N\partial\varepsilon_N(0)/\partial t$. Fourier analysis shows that ν_- is also diagonal in k-space, so that there is no excited-state contribution. We have $E_2(0, N) = N\varepsilon_N(0)$ for $N = 4n + 2$ and diamagnetic ring currents that scale as

N. The $k = \pm\pi/2$ levels of $4n$ rings are half-filled. The ground-state energy has a linear contribution in H and its curvature diverges. The divergence attenuates as $1/N$, with diamagnetic ν_+ contributions from $4n-2$ filled orbitals. Infinite Hückel rings are diamagnetic in the same sense that infinite Heisenberg chains have $S=0$ ground states without specifically excluding an odd number of spins.

For strong correlation ($z \gg 1$), $|G(z,N)\rangle$ is in the covalent subspace[2] with an electron localized on each site. Low-energy excitations are associated with spin flips, high-energy excitations $U_e = U - V$ with adjacent electron-hole pairs. The spin states of eq. (1) for large z are given by a Heisenberg antiferromagnetic chain.

$$H_e = \sum_p 2J\,(s_p \cdot s_{p+1} - 1/4), \tag{7}$$

with $J = 2t^2/U_e$. Virtual electron-hole excitation stabilize antiparallel spins, but are excluded for parallel spins.

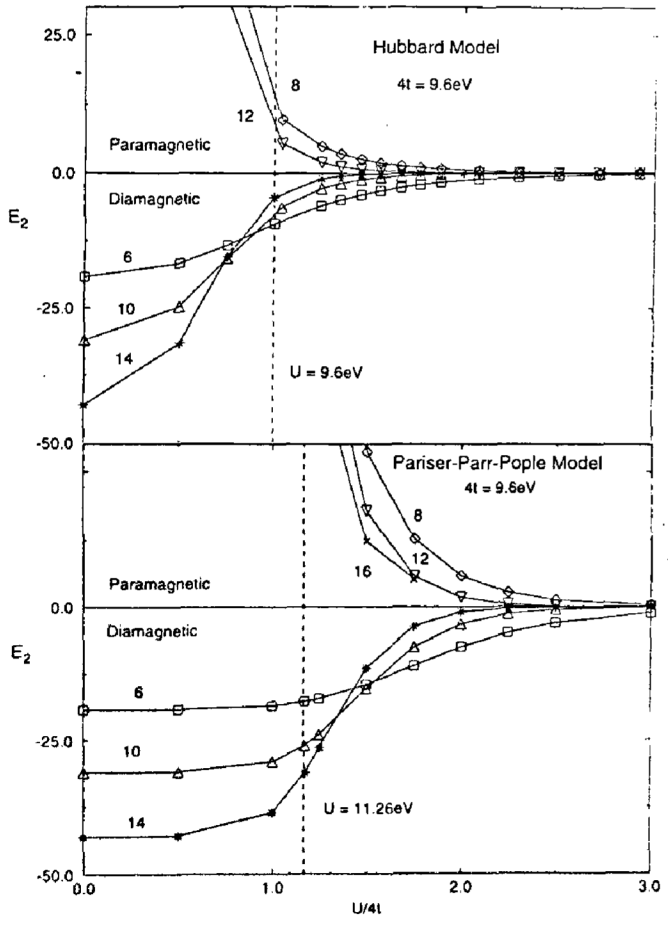

Figure 1. Exact ring currents of regular annulenes, from $N=6$ to 16 sites, with bandwidth $4t = 9.6$ eV and variable U in Hubbard and Pariser–Parr–Pople models. The ground-state correction E_2, eq. (5) in eV, is proportional to ring currents. I_N is diamagnetic for $4n+2$, paramagnetic for $4n$, and vanishes at large $z = U/4t$; $U = 11.26$ eV is the PPP choice for conjugated hydrocarbons.

The ground-state energy per site, $\varepsilon_N(J)$, is $-2J\ln 2$ for the infinite chain[13]. The ν_+ or bond-order contribution to eq. (5) is then $2N\varepsilon_N(J)$ and decreases with increasing z, as illustrated in Figure 2 for 14-site PPP rings.

The excited-state contribution to E_2 is the ground-state expectation value of

$$H' = \sum_k \frac{\nu_- |k\rangle\langle k|\nu_-}{E_k - E_0}. \tag{8}$$

Except for having ν_- instead of ν_+, H' is identical to the analysis[14] leading to eq. (7). For $z \gg 1$, we have intermediate states with $E_k - E_0 = U_e$. Excitations out of the covalent ground state are immediately annihilated, so that only left/right and right/left transfers are possible. These involve cross terms that have opposite signs in ν_-^2 and ν_+^2. We conclude that $H' = -H_e$ under precisely the same conditions. The excited-state contribution is consequently

$$2t^2 \sum_k |\langle k(z,N)|\nu_-|G(z,N)\rangle|^2/(E_k - E_0)$$
$$= -2\langle G|H_e|G\rangle = -2N\varepsilon_N(J). \tag{9}$$

The paramagnetic contribution to I_N cancels the bond-order contribution at least to order $(t/U_e)^3$. The next correction has four transfers and its structure has not been analysed. Rapid convergence to $E_2 = 0$ for $z > 1$ follows for any $V(R)$ in eq. (1) whose atomic limit is H_e. Excited-state contributions in $4n$ rings exceed the ground-state term and converge to $I_N \sim 0$ in Figure 1 from the paramagnetic side for $N = 8$, 12 or 16.

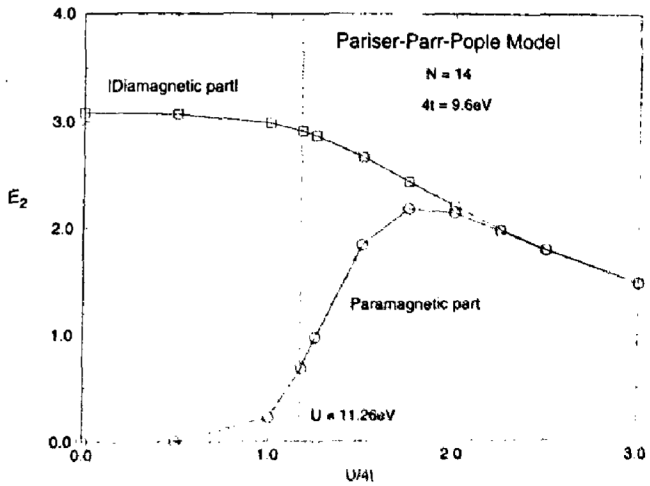

Figure 2. Magnitudes of E_2 contributions for a regular 14-site annulene using the Pariser–Parr–Pople model. The diamagnetic part is the ground-state or ν_+ term in eq. (5); the paramagnetic part is the excited-state or ν_- term; $U = 11.26$ eV is the PPP choice for hydrocarbons.

Aromatic stabilization and conjugated molecules

Figure 3 shows the ground-state energy per site, $\varepsilon_N(z) = E_0(z, N)/N$, of PPP rings. As noted in eq. (6), $4n$ Hückel rings converge as N^{-2} from above, $4n+2$ rings from below. Standard PPP parameters ($U = 11.26$ eV, $R = 1.397$ Å, the benzene bond length) follow the same pattern: $\varepsilon_N(z)$ gives excellent N^{-2} fits for $4n$ and $4n+2$. But the lines apparently intersect at N_c ($z = 1.173$) ~ 25, as marked by the arrow in Figure 3, although the actual merging is smooth. We expect the sequences to coincide for $N > N_c$. Stronger correlations reduce the slopes and $N_c(z)$ in Figure 3 in the $z \gg 1$ limit, $\varepsilon_N(J)$ for Heisenberg rings converge as N^{-2} with $4n$ and $4n+2$ falling on the same line, as is already evident at $U = 25$ eV. The corresponding I_N in Figure 1 is very small. The $4n, 4n+2$ energies merge at $U = 17$ eV around $N_c = 14$, in the crossover region to small I_N. Although finite-size effects persist for $z > 1$, the distinction between aromatic and antiaromatic behaviour in regular annulenes disappears around $N_c(z)$ using either an energy or ring-current criterion.

The correlation cross-over of regular annulenes at $N_c(z)$ corresponds to the merging of $4n, 4n+2$ ground-state energies. Since $4n, 4n+2$ annulenes are paramagnetic and diamagnetic, respectively, vanishing I_N is virtually required for large z. The situation for weak correlations is different, however, since infinite Hückel rings are strongly diamagnetic. We show in the Discussion that extended systems have a critical z_c that marks the boundary between diamagnetic I_N for $z < z_c$ and vanishing ring currents for $z > z_c$. The correlation transition is interesting in the context of models. The stabilization energy is a small correction to $E_0(z, N)$ at $z = 0$, while I_N or E_2 are extensive in N. The size dependence of stabilization and I_N is entirely different in regular annulenes. There is no stabilization in the infinite chain, the usual reference for aromaticity, whose I_N formally diverges in Hückel theory.

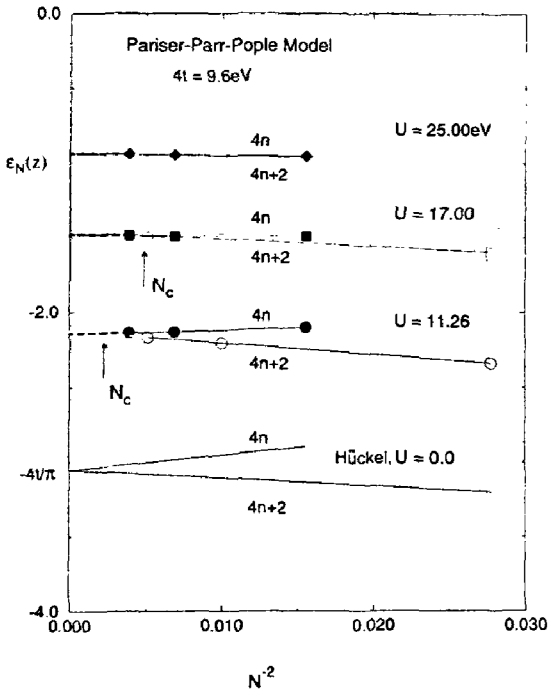

Figure 3. Exact ground-state energy per site $\varepsilon_N(z)$, eq. (3) in eV, of regular annulenes from $N = 6$ to 16 sites using the Pariser–Parr–Pople model with the indicated $z = U/4t$. The N^{-2} convergence of $\varepsilon_N(0)$ is exact. The $4n, 4n+2$ sequences for $U > 0$ merge at the indicated $N_c(z)$ and fall on a common line for $U = 25$ eV or larger.

Hubbard or PPP models of regular annulenes focus on intrinsic π-electronic properties, without physical constraints such as bond angles or instabilities. Conjugated molecules are far more complicated: $4n+2$ annulenes with $n = 4, 5$, or 6 are planar but not regular and the Peierls instability to partial single and double bonds sets in around[5] $N = 30$. Cyclobutadiene is rectangular, while cyclooctatetraene is a tub. Ring currents and stabilization in conjugated molecules are less clear cut than in models and less instructive in some sense. But physical systems in turn constrain models through the appropriate $V(R)$.

Thus π–π^* spectra of conjugated hydrocarbons unequivocally favor long-range $V(R)$ over Hubbard or extended Hubbard models. Standard PPP parameters $U = 11.26$ eV for carbon, $|t| = 2.40$ eV are marked in Figures 1 and 2. When combined with CC bond lengths, the PPP model predicts π-electronic excitations of hydrocarbons and neutral states of conjugated polymers, including transition moments and nonlinear optical responses[1,2]. Polyenes, polyacenes, stilbene and pyrene[11] illustrate the power of exact PPP results with transferable parameters. These molecules and many conjugated polymers are alternant or bipartite, with all π-bonds connecting sites in two sublattices. The half-filled ($N_e = N$) case has electron-hole symmetry when all site energies (Hückel α) are identical. The charge distribution is then uniform[2], with $n_p = 1$ for all p in any eigenstate of (1).

Pyracylene (Figure 4) is nonalternant due to its five-membered rings and thus provides a different test. The standard D_{2h} structure is uniquely defined by $R = 1.397$ Å for all bonds and 120° bond angles of hexagons. This fixes t and $V_{pp'}$ in eq. (1) for $N = N_e = 14$. The π-electron charge densities and bond orders in the ground state are given in Figure 4. The five lowest odd-parity singlets, their symmetry and oscillator strength are listed in Table 1. Dipole-allowed excitations to B_{2u} or B_{3u} states are x or y polarized, respectively. Two-photon excitations are A_g or B_{1g} singlets with two parallel or perpendicular transition dipoles, respectively.

The experimental results in Table 1 are based on hexane solution and stretch-oriented sample[15]. The weak

2.56 eV signal was not assigned. Its oscillator strength is about 100-fold less than the x-polarized feature at 2.90 eV, which in turn is about 5-fold less intense than the y-polarized feature at 3.46 eV. There is absorption in both polarization around 4 eV, as calculated, and assignments are tentative. Overlapping vibronic progressions complicate the analysis. Their incorporation into PPP or other models remains a challenge. The linear absorption in Table 1 agrees well with experiment, in contrast to self-consistent (approximate) PPP results[15] that get the parity of the weak state wrong and greatly overestimate the y-polarized intensity. Two-photon excitations have not been reported. We find the lowest singlet at 0.62 eV (B_{1g}), the second singlet at 1.93 eV (A_g). Modest improvements can be expected for the actual pyracyclene structure, taken either from crystal data, bond-order bond-length correlations, or quantum chemical calculations. The pentagon bond orders in Figure 4 clearly indicate a double and two single bonds, and thus modified bond lengths and $t(R)$.

Pyracylenes are embedded in the larger conjugated surface of C_{60}. The fragment is then not planar. PPP[16] and Hartree–Fock[17] calculations show paramagnetic ring currents in the five-membered rings, diamagnetic ring currents in six-membered rings, and overall diamagnetism. This C_{14} molecule has a C_{12} periphery. The periphery of polycyclic aromatics[8] usually governs the magnetism or ring currents, but not in this case.

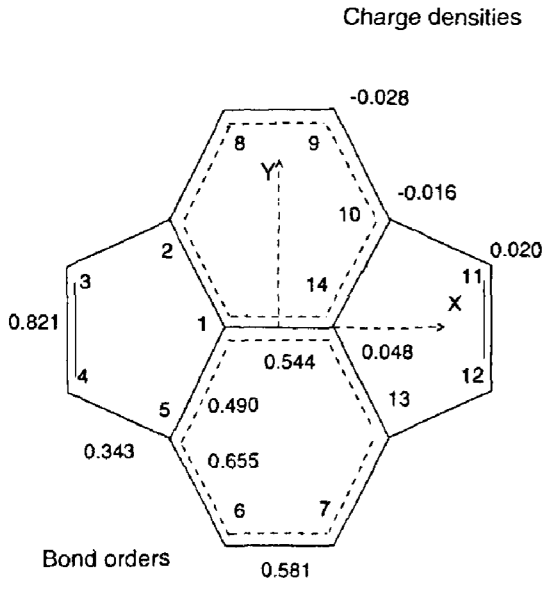

Figure 4. *Schematic* representation of pyracylene conjugation and exact π-electron bond orders and charges densities in Pariser–Parr–Pople ground state. The ideal D_{2h} structure has equal bonds $R = 1.397$ Å and hexagons with 120° bond angles. Finite π-charges are due to nonalternant connectivity; the bond orders indicate single, double, and partial π-bonds as shown.

Discussion

Chemical shifts obtained by NMR probe local magnetic fields directly. There are other sources than ring currents, however, and assessment of all contributions[18] requires accurate molecular wave functions and rather small systems. Quantum cell models are obviously simpler but less physical. As seen in Figure 1, I_N doubles between $N = 6$ and 14 in PPP rings with standard parameters. Increased diamagnetism of annulenes goes with decreased aromatic stabilization in Figure 3. The crossover $I_{14} = I_{10}$ occurs at larger than physical U. We expect somewhat larger I_{18} for standard parameters, with the I_{18}/I_{14} crossover still above $U = 11.26$ eV. The trend in Figure 1 suggests decreasing I_N in larger annulenes. The largest proton shifts[19] occur in 18-annulene, about 10% higher than 14-annulene and almost twice 26-annulene. As noted previously[9], PPP analysis of regular annulenes accounts naturally and semiquantitatively for these shifts.

Charged annulenes have considerably larger chemical shifts[19] than neutral ones, contrary to the single-particle result that I_N is maximized at $N_e = N$ and decreases on removing electrons from bonding orbitals or adding them to antibonding orbitals. Larger I_N for $N_e \neq N$ follows in general for correlated states. For $z \gg 1$, the models (1) reduce to noninteracting spinless fermions. The lower Hubbard band is filled in neutral ($N_e = N$) annulenes and I_N vanishes. But ring currents for $q = N_e - N$ electrons or holes go as $t \cos k$ and remain finite. Standard PPP parameters yield[9] larger I_{14} for $q = \pm 4$ than $q = 0$; the difference is an order of magnitude by $U = 17$ eV. The electron-hole symmetry of the model ensures identical E_2 for anions and cations, but I_N could differ due to the area S in eq. (4). Multiples of $q = 4$ retain closed shells in $4n + 2$ annulenes, while $q = 2$ yields closed shells in $4n$ annulenes and rationalizes planar cyclooctatetraene dianions. Chemical constraints sharply limit direct comparisons of charged and neutral molecules.

The correlation transition of infinite annulenes is a new result for quantum cell models. Diamagnetic I_N reflects ground-state precession of all π-electrons. The current per electron is proportional to E_2/N, which is shown in Figure 5 for PPP models. The Hückel limit is given by $4n + 2$ annulenes, when the bond-order

Table 1. Linear absorption of pyracylene: Exact PPP excitation energies and oscillator strengths

Symmetry	Energy (eV)	Expt[a] (eV)	f[b]
B_{2u}	2.496	2.56	0.0004
B_{2u}	3.134	2.90 (x)	0.02
B_{3u}	3.376	3.46 (y)	0.10
B_{2u}	4.321	3.87 (x)	0.06
B_{3u}	4.322		0.10

[a] Hexane solution, 298 K, ref. 15.
[b] Oscillator strength, $f = 1.085 \times 10^{-5} \nu |\mu|^2$, ref. 8, p. 358.

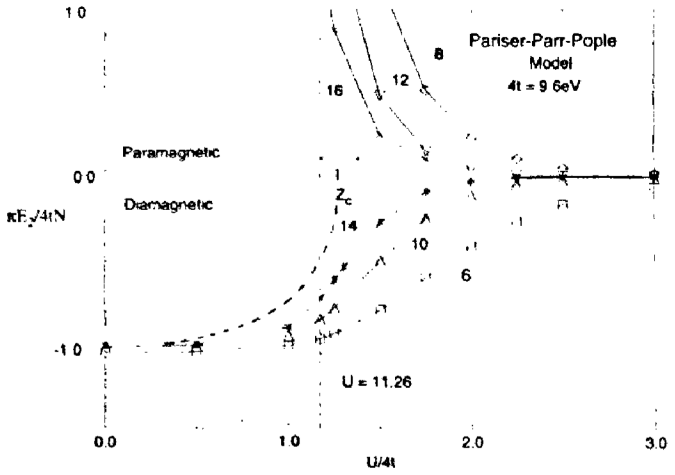

Figure 5. Exact ring currents per site, or E_2/N in eq. (5), in Pariser–Parr–Pople models of regular N-site annulenes with increasing $z = U/4t$. The infinite chain has diamagnetism $\pi E_2/4tN = -1$ at $z = 0$, follows the dashed line discussed in the text, and has a correlation transition to a nonmagnetic state at z_c, estimated to be slightly above the physical $U = 11.26$ eV.

contribution in eq. (5) dominates the $k = \pi/2$ degeneracy of $4n$ rings. The convergence of E_2/N in Figure 5 indicates diamagnetism for $z < 1$ and vanishing I_N for $z > 1$. The critical $z_c \sim 1.2$ and dashed line in Figure 5 are rough estimates of the correlation transition to a nonmagnetic state. We expect more accurate z_c when $N = 18$ results become available and additional analysis is performed on the shape of $E_2(z, N)$. The dashed line for $N \to \infty$, $-\pi E_2(z, N)/4tN$, is the order parameter for diamagnetism. It rigorously starts at $\pi\varepsilon_\infty(0)/4t = -1$, remains near the $N = 14$ curve up to $z \sim 1/2$, deviates upward at higher z and has discontinuous slope at z_c. The critical correlation of Hubbard chains is lower, around $z_c \sim 0.8$. We expect finite z_c for any potential $V(R)$ leading to spin-charge separation and H_e. The correlation transition of regular annulenes separates macroscopic diamagnetism from a nonmagnetic state.

Vanishing ring currents at z_c are reminiscent of Mott or metal–insulator transitions. Both are associated with narrow half-filled bands and both give currents for $N_e \neq N$, but the currents are due to static electric and magnetic fields, respectively. The half-filled Hubbard chain has a finite gap for any $z > 0$ and does not have a Mott transition[20] since a finite energy gap defines an insulator. Finite gaps for charged excitations are expected for other $V(R)$ in eq. (1) when $N_e = N$, but there are no exact results. By contrast, all electrons contribute to ring currents and substantial correlation $z \sim 1$ is needed to suppress I_N, as shown in Figure 5 for PPP rings. Moreover, diamagnetic I_N in $4n + 2$ annulenes is compatible with finite-size gaps. Thus small I_N is associated with spin-charge separation rather than an energy gap. The cross-over to vanishing I_N becomes narrower with increasing N, as expected. We anticipate sharp correlation transitions at $z_c \sim 1$ in infinite Hubbard, PPP or related chains whose atomic limit is a Heisenberg antiferromagnetic chain. As in Mott transitions, the ground state changes qualitatively. The correlation transition from diamagnetic to nonmagnetic ground state remains to be characterized accurately and illustrates how simple models connect entirely different molecular and solid-state properties.

1. Soos, Z. G., Painelli, A., Girlando, A. and Mukhopadhyay, D., in *Handbook of Conducting Polymers* (eds Skotheim, T. A., Elsenbaumer, R. and Allen, T.), Marcel Dekker, New York, 1997, p. 165 and references therein.
2. Soos, Z. G. and Ramasesha, S., in *Valence Bond Theory and Chemical Structure* (eds Klein, D. J. and Trinajstic, N.), Elsevier, Amsterdam, 1989, p. 81; Soos, Z. G., Galvão, D. S. and Etemad, S., *Adv. Mat.*, 1994, **6**, 280.
3. Berson, J. A., *Angew. Chem. Int. Ed. Engl.*, 1996, **35**, 2750.
4. Longuet-Higgins, H. C. and Salem, L., *Proc. R. Soc. London*, 1959, **A251**, 172.
5. Choi, C. H. and Kertész, M., *J. Chem. Phys.*, 1998, **108**, 6681, and references therein.
6. London, F., *J. Phys. Radium*, 1937, **8**, 397.
7. Krishnan, K. S., Guha, B. C. and Banerjee, S., *Philos. Trans. R. Soc. London*, 1933, **A213**, 235; Krishnan, K. S. and Banerjee, S., *ibid*, 1935, **A234**, 265.
8. Salem, L., *The Molecular Orbital Theory of Conjugated Systems*, Benjamin, New York, 1966, ch. 4.
9. Kuwajima and Soos, Z. G., *J. Am. Chem. Soc.*, 1987, **109**, 107.
10. Ohno, K., *Theor. Chim. Acta*, 1964, **2**, 219.
11. Wen, G. and Soos, Z. G., *J. Chem. Phys.*, 1998, **108**, 2486.
12. Ramasesha, S. and Soos, Z. G., *Chem. Phys. Lett.*, 1988, **153**, 171; *J. Chem. Phys.*, 1989, **90**, 1067.
13. Hulthén, L., *Arkiv. Mat. Astron. Fysik*, 1938, **26A**, No. 1.
14. D. C. Mattis, *The Theory of Magnetism*, Harper and Row, New York, 1965, p. 186; Van Vleck, J. H., in *Quantum Theory of Atoms, Molecules and the Solid State* (ed. Löwdin, P. O.), Academic, New York, 1966, p. 475.
15. Freiermuth, B., Gerber, S., Riesen, A., Wirz, J. and Zehnder, M., *J. Am. Chem. Soc.*, 1990, **112**, 738.
16. Chakrabarti, A., Anusooya, Y. and Ramasesha, S., *J. Mol. Struct. (Theochem.)*, 1996, **361**, 181.
17. Fowler, P. W., Zanasi, R., Cadioli, B. and Steiner, E., *Chem. Phys. Lett.*, 1996, **251**, 132.
18. Chesnut, D. B., in *Reviews in Computational Chemistry* (eds Lipkowitz, K. B. and Boyd, D. B.), VCH Publishers, New York, 1996, p. 245.
19. Müllen, K., Huber, W., Meu, T., Nakagawa, M. and Iyoda, M., *J. Am. Chem. Soc.*, 1982, **104**, 5403.
20. Lieb, E. H. and Wu, F. Y., *Phys. Rev. Lett.*, 1968, **20**, 1445.

ACKNOWLEDGEMENTS. We thank R. A. Pascal, J. S. Siegel and K. M. Mislow for discussions of aromaticity and the National Science Foundation for supporting this work through DMR-9530116.